

Study on a Low Complexity ECG Compression Scheme with Multiple Sensors

Pengda Huang

Abstract—The industry of wearable remote health monitoring system keeps growing. In the diagnosis of cardiovascular disease, Electrocardiography (ECG) waveform is one of the major tools which is thus widely taken as the monitoring objective. For the purpose of reducing bit expenditure in the monitoring systems, we study the compression of ECG signal and propose a new compressor in low complexity. Different from the traditional ECG compressors, most of which are built on a single sensor, our compression scheme is based on multiple ECG sensors. The multi-sensor based compression scheme is able to provide more accurate sensing results. Besides the investigation into the structure of the compressor, we also jointly optimize the period and the bit number per sample in the transmission of ECG signal. Experiments are performed on records in MIT-BIH Arrhythmia database and European ST-T database. Experimental results show that our method outperforms conventional ones with respect to ECG reconstruction accuracy at the same bit rate consumption.

I. INTRODUCTION

Thanks to the development of mobile communication and positioning technologies [1]–[3] in the past several decades, remote health monitoring technology is near to practical application in our everyday life. ECG signal is one of the main tools of diagnosing cardiovascular diseases which are the major mortality causes in current societies, especially in developed countries. Remotely monitoring ECG signal provides an effective approach to avoiding the mortality caused by abrupt seizure of cardiovascular diseases.

Basically, in a remote monitoring system a wearable device collects biomedical information, and transmit the collected information to a remote data unit for prompt or delayed diagnosis. The remote monitoring relies on the transmission of the bits which carry ECG signal. The bit transmission induces cost due to consumption of resources provided by infrastructures in mobile communication systems. For the purpose of reducing the cost, we investigate how to reduce the cost with respect to the two aspects, lowering the complexity of ECG compressor and reducing the rate of bits conveying ECG signal. The cost reduction efforts are under the prerequisite that the accuracy of the received ECG signal at the remote data unit should be under control and not degrade the diagnosis of cardiovascular diseases.

In literature, a single sensor is widely used to monitor ECG signal. In this paper, we consider multiple-sensor based ECG compression scheme. Generally, a multiple sensors based monitoring system provide more accurate and prompt sensing results since the sensors equipped at different places of our body are able to monitor the conditions of different parts of a heart. Fig. 1 presents an example of our proposed ECG

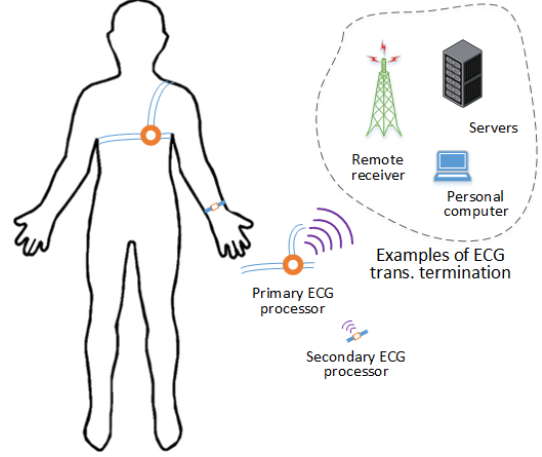


Fig. 1. Demonstration of two ECG signal compression scheme

compressor built on two sensors, a primary ECG sensor and a secondary sensor. As an arbitrary example shown in Fig. 1, the secondary sensor is put on the wrist which compresses ECG signal and the transmit the compression results to the primary sensor shown in the breast part. Battery capacity and computation capability of the secondary sensor are at a lower than the primary one since the targeted transmission distance of the secondary sensor is shorter. The primary sensor compresses and sends out the ECG signal from the secondary one and itself to a remote data center.

No matter a single- or multiple-sensor based monitoring system, energy consumption is widely recognized as a major concern [4]. The energy consumption is affected by diverse factors, such as hardware chip, circuit board design, encoder, modulation, or even selection of radio frequency (RF) antenna. Thus, we can hardly evaluate the energy consumption in all terms of the mentioned and unmentioned factors. Independent of the diverse factors, rate of the bits carrying the ECG signal provides us an effective approach to evaluating the energy consumption at a high level.

Single-sensor based ECG compression scheme have been studied in [5]–[14]. Basically, compression methods can be divided into two categories, direct and differential ECG compression methods.

Uniform quantization is basic one of the direct ECG signal compression methods. In [8], discrete cosine transform (DCT) was used to compress ECG signal. Similarly, DCT is also used in ECG signal compression [9] while Huffman coding was used to compress DCT results further. Still as a direct compression method, wavelet transform followed by run length coding was taken to compress ECG signal in [10], [11]. Compressive sensing was utilized to compress ECG signal in [12]–[14].

The compression of ECG signal is implemented in differential structures. Differential schemes built on a linear prediction model are used to compress ECG signal in [15], [16]. Multiple ECG samples in the past are taken to predict ECG value in one step ahead. Then, the difference between the prediction and its real value is quantized. In [7], [17], [18], adaptive signal processing methods are taken to update the coefficients of the linear prediction model.

We observe that adjacent ECG samples are not independent to each other. The dependence means there exists redundant information between the samples. Differential compression can effectively reduce the redundant information. After the redundant information reduction, less bits are needed for the quantization. Therefore, differential ECG compression is taken as one of the research objectives in this paper.

There is an important but not solved problem in existing differential ECG compression methods. As we know, coefficients of an adaptive filter for predicting a stationary signal do not change versus time. However, ECG signal is not stationary. Furthermore, ECG signals from a same person can be significantly different. Let us consider such a scenario that one person, sitting on a bench for a long time, stands up to leave. The period of R-R waves in ECG waveform will be different before and after his or her status transition, from sitting to walking. In this case, coefficients of the adaptive filter for predicting his or her ECG waveform will also be different. To keep ECG reconstruction at a high fidelity, the coefficients need to be recalculated and retransmitted; otherwise, there will be huge reconstruction error. To transmit the coefficients of an adaptive filter, a large number of bits will be consumed which is thus harmful to ECG transmission efficiency. In [7], [15]–[18], adaptive filters based differential ECG compression schemes are investigated. In their compression schemes, either updating or transmitting coefficients of adaptive filters may cause significant increase of computation resources.

Different from the existing ECG signal compression schemes, we proposed a new structure which is built on multiple ECG sensors. The proposed ECG compressor is at a low complexity. More specifically, the contributions in this paper are presented as follow,

First, we investigate ECG signal compression system with multiple sensors. Simple superposition of multiple sensors is not considered. From a same person, the ECG signals acquired by different ECG sensors at the same time instant usually have similarity in waveform shapes. The similarity means the redundant information. After realizing the signal redundancy between ECG sensors, we design a new ECG compression scheme which effectively saves the bits by reducing the redundancy.

Second, we propose a novel differential ECG compression scheme which is implemented via comparison and addition operations, and free of multiplications. The traditional differential ECG compressors are built on adaptive filters which rely on the updating filter coefficients and thus increase resource consumptions. This problem does not exist in our compression scheme. Furthermore, we optimize the codebook used for compressing the differential ECG signal.

Third, we optimize compression ECG compression bit rates

in two dimensions, the sampling period and the number of bits per sample. To my best knowledge, bit number per sample was considered in literature while the joint optimization is absent.

The remainder of this paper is organized as follows. In Section II, the potential problems of the existing compression methods will also be analyzed. In Section III, a novel ECG compression scheme built on multiple sensors will be presented. The joint optimization of bit rate over quantization level and sampling period will be performed in Section IV. Experiments and simulations will be presented in Section V which are followed by conclusions in Section VI.

II. RELATED WORK AND POTENTIAL PROBLEMS

In this section, we investigate the potential problems in the existing differential ECG compression schemes. Due to the large number of existing reports on ECG compression, our study will not cover all methods but only target at several typical ones.

A. Open-loop Predictive ECG Compression

1) *Open-loop based differential ECG compression method:* Finite impulse response (FIR) predictor was widely used in the open-loop based ECG compression. One example of the ECG compressors is shown in Fig. 2.

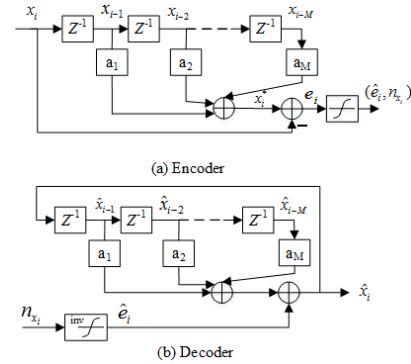


Fig. 2. Block diagram of open loop differential ECG compressor

Let $x(t)$ denote the time continuous ECG signal to be compressed and x_i denote periodical samples of $x(t)$, $i \in \mathbb{Z}$. Assume the FIR predictor is in the order of M . Let a_m , $m \in \{1, 2, \dots, M\}$ denote coefficients of the predictor. At the i -th time instance, estimation of ECG signal is denoted by x_i^* which is calculated as follows

$$x_i^* = \sum_{m=1}^M a_m x_{i-m}. \quad (1)$$

Estimation error between x_i^* and x_i is determined by

$$e_i = x_i^* - x_i. \quad (2)$$

In a differential ECG signal compression scheme, the estimation error e_i should be encoded and transmitted to a remote receiver. The receiver decodes the codewords and obtains the reconstruction of e_i , which is denoted by \hat{e}_i . With \hat{e}_i , ECG

signal is reconstructed by

$$\hat{x}_i = \hat{e}_i + \sum_{m=1}^M a_m \hat{x}_{i-m}. \quad (3)$$

The major concern for the open-loop based differential ECG compressor is the stability at the decoder. If errors in quantizing e_i will be accumulated, the compressor system is unstable. Unfortunately, there was no attention paid to the stability problem for open-loop compressors.

2) *Stability of open-loop based differential ECG compression*: An unstable open-loop compressor will accumulate quantization errors which will eventually cause the failure of ECG signal reconstruction at the decoder. Therefore, we need to analyze the quantization error accumulation problem at the decoder side. As defined in Section II-A1, e_i is the difference between x_i and its estimation \hat{x}_i^* . At the decoder side, the difference between x_i and its reconstruction \hat{x}_i is denoted by e_i^* ,

$$e_i^* = x_i - \hat{x}_i. \quad (4)$$

Furthermore, we define e_{qi} as the difference between e_i and \hat{e}_i ,

$$e_i = \hat{e}_i + e_{qi}, \quad (5)$$

where e_{qi} is essentially the quantization error in compressing e_i .

We can realize that e_i^* measures the bias of the reconstructed ECG sample with respect to its real value. Only if e_i^* stays within a small bounded range, the decoder is able to obtain accurate ECG samples. The quantization error e_{qi} is the factor which may cause e_i^* to be outside of the bounded range. Therefore, we construct e_i^* as a function of e_{qi} . Via analyzing the stability of the function, we can understand whether the ECG compressor is stable. The function is derived as follows,

$$\begin{aligned} e_i^* &\stackrel{(a)}{=} x_i - \left(\sum_{m=1}^M \hat{x}_{i-m} a_m + \hat{e}_i \right) \\ &\stackrel{(b)}{=} x_i - \left(\sum_{m=1}^M \hat{x}_{i-m} a_m + e_i - e_{qi} \right) \\ &\stackrel{(c)}{=} x_i - \left(\sum_{m=1}^M \hat{x}_{i-m} a_m + x_i - \hat{x}_i^* - e_{qi} \right) \\ &\stackrel{(d)}{=} \sum_{m=1}^M (x_{i-m} - \hat{x}_{i-m}) a_m + e_{qi} \\ &\stackrel{(e)}{=} \sum_{m=1}^M e_{i-m}^* a_m + e_{qi}, \end{aligned} \quad (6)$$

where (a) follows (3); (b) follows (5); (c) follows (2); (d) follows (1); and (e) follows (4).

We calculate z transformation of (6) as follows,

$$H_{OLP} = \frac{\mathbf{Z}\{e^*\}}{\mathbf{Z}\{e_q\}} = \frac{1}{1 - \sum_{m=1}^M a_m z^{-m}}, \quad (7)$$

where $\mathbf{Z}\{\cdot\}$ denotes the operator of Z transformation.

The stability of (7) depends on coefficients a_m , $m \in \mathcal{M}$. Indeed, shapes of ECG waveforms will differ with different

people or different health conditions. The change of ECG waveform generates the different a_m . Furthermore, the inconsistency of a_m means no guarantee of the stability in (7).

Aligning with the work in literature, we consider 4-th order FIR predictor. Under MMSE rule, the two sets of $\{a_m\}$ corresponding to No. 106 and No.118 ECG records are equal to $\{-0.1436, -0.2120, 0.1582, 1.1548\}$ and $\{-0.2276, -0.2041, 0.2512, 1.1761\}$ respectively. With the calculated coefficients, $H_{OLP|a}$ and $H_{OLP|b}$, are correspondingly determined. Then, poles of the two impulse response functions are calculated which are equal to $p_a = \{-0.9823, -0.0761 \pm j1.0866, 0.9908\}$ and $p_b = \{-0.9868, -0.1200 \pm j1.0856, 0.9991\}$ respectively. From the poles, we can easily realize that $H_{OLP|a}$ and $H_{OLP|b}$ are not necessary to be stable which means there exists the risk of inducing the failure of ECG reconstruction at the decoder.

B. Closed-Loop Predictive ECG Compression

From Section II-A2, open-loop differential ECG compressors have the risk of being instable at the decoder. This problem can be solved by adding a feedback to the quantization of e_i .

1) *Closed-loop differential ECG compression method*: The differential compressor with a feedback is called as closed-loop differential ECG compressor. Still M denotes the order of the linear model used to estimate the value of an ECG sample. When $M = 1$, the differential compressor degenerates into Differential pulse code modulation (DPCM).

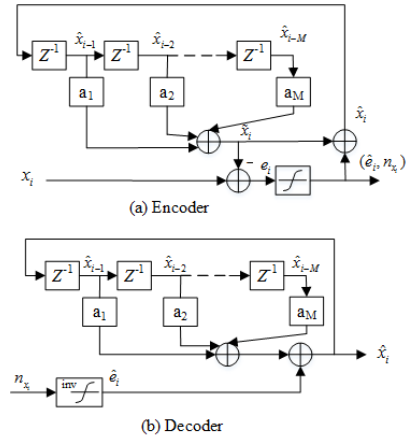


Fig. 3. Block diagram of closed loop differential ECG compressor

Fig. 3 plots the block diagram of closed-loop differential compressors. Compared with open-loop compressor, the major difference in the closed-loop one is that reconstruction is performed at the encoder side, and the reconstructed sample is taken as a reference of modifying the threshold for quantizing the next ECG sample.

Let \hat{x}_i denote the estimation of ECG sample at i -th time instance at the encoder side which is calculated by

$$\hat{x}_i = \sum_{m=1}^M a_m \hat{x}_{i-m}. \quad (8)$$

The estimation bias e_i is determined as follows,

$$e_i = x_i - \tilde{x}_i. \quad (9)$$

Afterwards, e_i is first quantized and the quantization result is denoted by \hat{e}_i , and the quantization error is still represented by e_{qi} . At the encoder side, the reconstruction of an ECG sample, denoted by \hat{x}_i , is obtained by adding the quantized e_i to \tilde{x}_i ,

$$\hat{x}_i = \tilde{x}_i + \hat{e}_i. \quad (10)$$

As shown in (10), \hat{x}_i is feed back to the input of the linear filter. Since \tilde{x}_i contains the error occurring in the quantization of the previous ECG sample, the feedback is beneficial for avoiding the accumulation of the quantization error.

2) *Stability of closed-loop based differential ECG compression*: Let e_{Ci}^* denote the difference between the ECG sample x_i and its reconstruction at the decoder. For closed-loop compressor, the reconstructions of an ECG sample at both the encoder and decoder are the same. Therefore, the reconstruction at the decoder is also denoted by \hat{x}_i . Due to the same reason mentioned in Section II-A2, we calculate e_{Ci}^* as a function of e_{qi} . Via analyze the stability of the calculated function, we can understand whether there exists the risk of accumulating quantization errors. The calculation of the function e_{Ci}^* of e_{qi} is presented as follows,

$$\begin{aligned} e_{Ci}^* &\triangleq x_i - \hat{x}_i \stackrel{(a)}{=} x_i - \left(\sum_{m=1}^M a_m \hat{x}_{i-m} + \hat{e}_i \right) \\ &= x_i - \left(\sum_{m=1}^M a_m \hat{x}_{i-m} + e_i - e_{qi} \right) \\ &\stackrel{(b)}{=} x_i - \left(\sum_{m=1}^M a_m \hat{x}_{i-m} + x_i - \sum_{m=1}^M a_m \hat{x}_{i-m} - e_{qi} \right) \\ &= e_{qi} \end{aligned} \quad (11)$$

where (a) follows (10); (b) follows (8) and (9).

From (11), ECG reconstruction error in the closed-loop compressor is fully determined by the error in quantizing e_i . In practice, quantization error is finite in a given quantizer. Therefore, the closed loop ECG compressor is always stable.

III. PROPOSED ECG COMPRESSION SCHEME BASED ON MULTIPLE SENSORS

Besides the absence of the stability analysis of ECG compressor, there is another unsolved problem in the existing studies, that is, only signal sensor is considered to compress ECG signal. Indeed, more sensors are able to provide more observations on the heart conditions since ECG signals obtained by sensors placed on different places of a body reflect the health conditions of different parts of a heart. Therefore, we investigate the ECG signal compression based on multiple sensors.

For multiple sensors, independent quantization is an inefficient practice since the redundancy between ECG signals from the multiple sensors is not removed. The retaining redundant information induces more bits for quantization. We propose a compression method used for multiple sensors.

The multiple sensors are divided into two tiers, that is, one primary sensor is taken as the first tier and the all the other sensors are at the secondary tier. The primary sensor has more powerful computation and transmission abilities which is responsible for remotely transmitting the ECG signal. The secondary sensors transmit their collected ECG signal to a primary one and the transmission range is smaller than that for the primary sensor. At the secondary sensor, conditional quantizer is used to compress ECG signal which can effectively reduce the redundant information. For analysis simplicity, we consider the case with one primary sensor and one secondary sensor.

A. Structure of Multiple Sensors Based ECG Compression Scheme

1) *System Overview*: Fig. 4 presents the block diagram of the compression scheme built on the primary sensor and secondary sensor. The secondary sensor transmits quantized ECG signal \hat{x}^S to the primary one. The primary sensor quantizes x^P to obtain \hat{x}^P and transmits the two quantized ECG signals (\hat{x}^S and \hat{x}^P) to a remote data unit. In the scheme, waveform features of \hat{x}^P are priorly known by the secondary sensor.

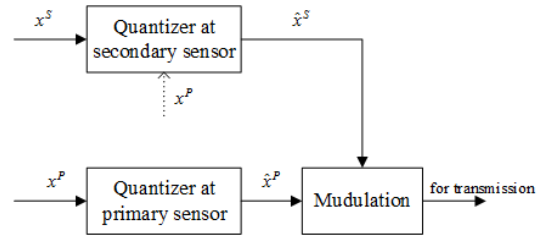


Fig. 4. Block diagram of double sensor quantization scheme

With the waveform feature of \hat{x}^P , we perform conditional quantization at the secondary sensor. The output from the conditional quantizer at the secondary sensor is sent to the primary one. The primary sensor takes differential compression scheme to quantize ECG signal.

After introducing the functions of the modules in the compression scheme, we present the details of how to implement the differential compression method at the primary sensor which is followed by the stability analysis. Then, the conditional quantization at the secondary sensor is introduced.

2) *Differential compression scheme at primary ECG sensor*: Block diagram of our proposed differential ECG compressor is presented in Fig. 5. Fig. 5 (a) and (b) describe the encoder and decoder respectively. Compared with conventional closed-loop compressors, only addition and comparison operations are needed, and multiplication is absent in the proposed one. Furthermore, we will illustrate our compressor outperforms the conventional ones in terms of ECG reconstruction accuracy.

In the new differential compressor, the difference between two adjacent ECG samples is first calculated as follows,

$$\Delta x_i = x_i - x_{i-1}. \quad (12)$$

Next, a modification factor, denoted by A , is added to Δx_i . The factor A is designed to counteract the accumulation

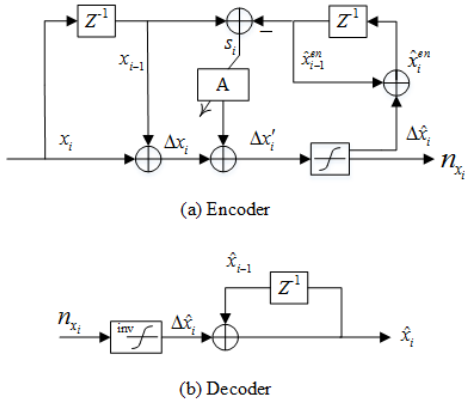


Fig. 5. Block diagram of proposed ECG data compression scheme

of quantization errors. After the addition of A , the adjacent difference Δx_i is derived into $\Delta x'_i$ as follows,

$$\Delta x'_i = \Delta x_i + A. \quad (13)$$

Afterwards, $\Delta x'_i$ is quantized and quantization index is denoted by l_i . The quantization levels constitute a set Φ , $\Phi = \{\phi_l, l \in \mathcal{L}\}$, $\mathcal{L} = \{1, 2, 3, \dots, L\}$, where N is equal to the total number of quantization levels. The elements in Φ are ordered incrementally. As we know, the set Φ has impact on the quantization performance. The details in designing Φ will be introduced in Section III-B2. After the quantizing $\Delta x'_i$, the compressor will perform modulation according to l_i .

From the previous paragraph, the modification factor A is an important parameter. Next, we discuss the details of how to determine A .

Let $\Delta \hat{x}_i$ denote the quantized $\Delta x'_i$. To reconstruct the ECG sample at i -th time instance (\hat{x}_i) at the encoder, we add the $\Delta \hat{x}_i$ to \hat{x}_{i-1} ,

$$\hat{x}_i = \hat{x}_{i-1} + \Delta \hat{x}_i. \quad (14)$$

Since A is used to counteract the accumulation of quantization error, A is designed to be a function for reducing the quantization error at the previous time instance. The quantization error at the previous time instance is calculated by

$$s_i = x_{i-1} - \hat{x}_{i-1}. \quad (15)$$

To avoid the accumulation of quantization error, A is set to be a small positive value, when $s_i < 0$; and A is a negative value, when $s_i \geq 0$. This correlation between A and $s_i < 0$ is mathematically described by

$$A = \begin{cases} \left(\phi_{l_{\Delta x'_i}} - \phi_{l_{\Delta x'_i}-1} \right) & \text{if } s_i > 0 \\ -\left(\phi_{l_{\Delta x'_i}+1} - \phi_{l_{\Delta x'_i}} \right) & \text{if } s_i < 0 \end{cases}, \quad (16)$$

where $l_{\Delta x'_i}$ denotes the index of the quantized $\Delta x'_i$ within the ordered set Φ , and $\phi_{l_{\Delta x'_i}}$ is the corresponding quantization result.

Stability Analysis: To analyze the stability of the proposed compression scheme, we derive the compression bias e_i^* as a function of the quantization error e_{qi} due to the same reason presented in Section II-A2. The quantization error e_{qi} satisfies

the following equation,

$$e_i' = \hat{e}_i + e_{qi}. \quad (17)$$

For analysis convenience, we simplify (16) into a form as follows,

$$A = \beta (x_{i-1} - \hat{x}_{i-1}), \quad (18)$$

where β is variable which absolute value is bounded into a small range and the sign of β is opposite to the sign of $(x_{i-1} - \hat{x}_{i-1})$.

Next, we determine the expression of e_i^* as follows,

$$\begin{aligned} e_i^* &= x_i - \hat{x}_i = x_i - (\Delta \hat{x}_i + \hat{x}_{i-1}) \\ &\stackrel{(a)}{=} x_i - (\Delta x_i + A - e_{qi} + \hat{x}_{i-1}) \\ &\stackrel{(b)}{=} x_i - (x_i - x_{i-1} + A - e_{qi} + \hat{x}_{i-1}) \\ &\stackrel{(c)}{=} (x_{i-1} - \hat{x}_{i-1}) - (\beta (x_{i-1} - \hat{x}_{i-1}) - e_{qi}) \\ &= \begin{cases} (1 - |\beta|) e_{i-1}^* + e_{qi} & \text{for } x_{i-1} - \hat{x}_{i-1} > 0 \\ (1 + |\beta|) e_{i-1}^* + e_{qi} & \text{for } x_{i-1} - \hat{x}_{i-1} < 0 \end{cases} \\ &= (1 - |\beta|) e_{i-1}^* + e_{qi}. \end{aligned} \quad (19)$$

where (a) follows (17) and (13); (b) follows (12); (c) follows (18).

The Z -transformation of (19) is written as

$$H(z) = \frac{\mathbf{Z}\{e^*\}}{\mathbf{Z}\{e_q\}} = \frac{1}{1 - (1 - |\beta|)z^{-1}}. \quad (20)$$

From (20), the pole is equal to $p = 1 - |\beta|$ which locates in inner of a unit circle. Therefore, our proposed ECG processor can avoid the accumulation of quantization error.

B. Quantizer Design in the Proposed ECG Compressor

In the optimum sense of minimizing average quantization error at a given number of quantization levels, the statistics of the quantization objective affects the design of an optimum quantizer. Thus, we first analyze the statistic features of the differential ECG signal. Afterwards, we present the details of how to design the differential ECG compressor. Then, the conditional quantization by the secondary sensor is introduced.

1) *Statistical Features of One-step Differential ECG Data:* There are two important issues determining statistical features of a signal, dynamic range of source and distribution of it. We will numerically analyze the differential ECG signal at the two aspects using two factors

Fig. 6 shows us the dynamical ranges of differential ECG and original ECG waveform which are calculated from 38 records in MIT-BIH database.

For each record, we calculate the maximum and minimum values of both original and differential ECG signals. All the extreme values are plotted in Fig. 6.

To determine the dynamical range of differential ECG signal, we first calculate the upper bound of the maximum points and lower bound of minimum points via linear interpolation. Afterwards, we perform curve fitting on the two bounds using two horizontal lines. The two horizontal lines label the boundaries of the differential ECG dynamical range. The same

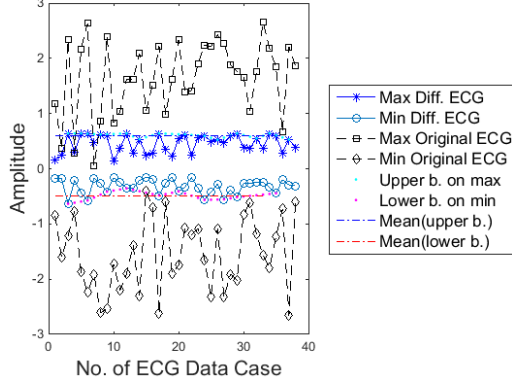


Fig. 6. Dynamical range of differential ECG and original ECG signal

method is also used to determine the dynamical range of the original ECG signal. From the calculation, we can observe that dynamical range of original ECG signal is approximately equal to 6. The differential ECG data has the dynamic range from -0.4854 to 0.6044. Since the dynamical range of the differential ECG signal is smaller than that of the original signal, less bits are needed for quantizing the differential ECG signal at a given quantization accuracy.

After analyzing the dynamical range, we study the distribution of the differential ECG signal. First, we calculate histogram of differential ECG signal which is plotted by the blue stars in Fig. 7. With the calculated histogram, we use the curve fitting technology to abstract an approximated probability model of the differential ECG signal.

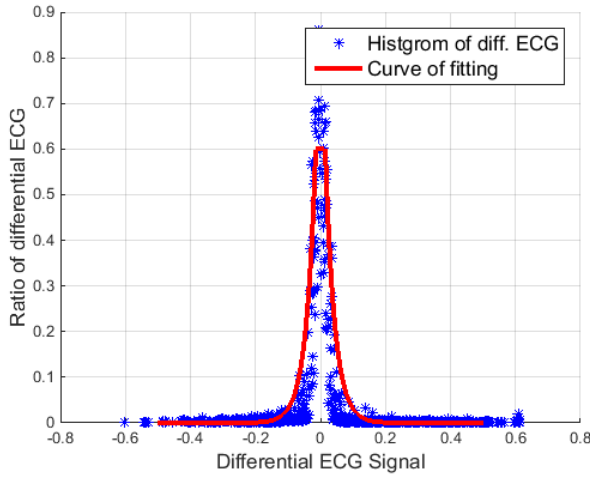


Fig. 7. Approximation of histogram via curve fitting using exponential functions

Let $f(\Delta x)$ denote the probability. An exponential function with peak clipping is used to represent the differential ECG histogram. The red bold curve in Fig. 7 plots the probability function $f(\Delta x)$ which takes a form of exponential function with the exponent of -50. With the calculated probability model, we analytically study the quantizer design in the following part.

2) *Quantization of differential ECG at primary sensor:* Assume the quantizer in our analysis is labeled by Q . The

quantizer is optimized in the sense of minimum mean square of quantization error. The mean square error is calculated by

$$esq_Q = \sum_{l=0}^{L-1} \int_{\Delta x_l}^{\Delta x_{l+1}} (\Delta x - \Delta x_l^0)^2 f(\Delta x) d\Delta x, \quad (21)$$

where L is the number of total quantization levels and x_l^0 is quantization output at l -th quantization level.

We select Lloyd-Max algorithm [19] to determine each quantization zone $(\Delta x_l, \Delta x_{l+1})$ and the value of quantization output Δx_l^0 . According to Lloyd-Max algorithm, the parameters are iteratively calculated as follows

$$\Delta x_l^0 = \frac{\int_{\Delta x_l}^{\Delta x_{l+1}} \Delta x f(\Delta x) d\Delta x}{\int_{\Delta x_l}^{\Delta x_{l+1}} f(\Delta x) d\Delta x}, \quad (22)$$

$$\Delta x_l = \frac{\Delta x_l^0 + \Delta x_{l+1}^0}{2}. \quad (23)$$

In a partial summarization of the quantization on the primary sensor, the histogram of the first order differential ECG signal is calculated first; second, via curve fitting, a PDF in an explicit form is calculate to approximate the histogram; third, the number of the bits for the quantization is determined; fourth, the codebook and quantization zones are determined according to (22) and (23) respectively.

3) *Quantization on the Secondary ECG Sensor:* The proposed differential ECG compression method at the primary sensor achieves the bit rate saving by reducing the redundancy between ECG samples from a same sensor. Besides, the redundancy within the ECG samples from a single sensor, there also exists inter-sensor redundancy which can be observed from the waveform similarities between the ECG signals from different sensors. Without loss of generality, No. 100 ECG recording in MIT-BIH arrhythmia database is plotted in Fig. 8 which is taken as an example of showing the existence of inter-sensor redundancy. We will reduce the inter-sensor redundancy to save the bit rate for the quantization on the secondary sensor.

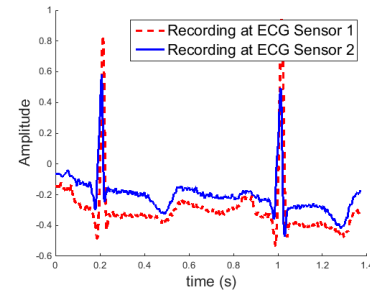


Fig. 8. Number 100 ECG recording in MIT-BIH Arrhythmia database

The ECG data collected by the primary sensor is denoted by x^P , and x^S is for the data from the secondary sensor. Let $f_P(\cdot)$ and $f_S(\cdot)$ denote the approximated PDFs from x^P and x^S respectively. At the secondary sensor, the approximated PDF of x^P is priorly known. The quantization based on the prior information is denoted by $Q(x^S|f_P)$.

Since there exists the connection between the waveforms of x^P and x^S , we build an affine relation between $f_P(\cdot)$ and

$f_S(\cdot)$. The affine is denoted by F which is determined as follows,

$$F = \{(a, b) | \min(f_P - a \cdot f_S - b)^2\}, \quad (24)$$

where a and b are constants for a group of ECG data from a same person, such as the group consisting of x^P and x^S .

With the established affine relation, the conditional quantization and codebook can be calculated according to the following four steps:

- First, a small number of bits, which number is denoted by N_1 , are used to quantize the support area of $f_S(\cdot)$. Since bits number is smaller, the quantization bins are sparse in the step. Let b_{1i}^S denote the i -th quantization bin. Boundaries of b_{1i}^S are x_{1i}^S and $x_{1(i+1)}^S$, where $x_{1i}^S \leq b_{1i}^S < x_{1(i+1)}^S$ and $i \in \{0, 1, 2, \dots, 2^{N_1}\}$.
- We calculate the boundaries x_i^P from x_i^S according to the F affine defined in (24). More explicitly, the calculation is presented below

$$x_i^P = a \cdot x_{1i}^S + b. \quad (25)$$

- Within each bin of b_{1i}^S , $i \in \{0, 1, 2, \dots, 2^{N_1}\}$, we utilize Lloyd-Max algorithm to calculate a sub-codebook which is denoted by c_i^S . Let N_2 denote the number of bits used in the sub-level quantization.
- Using the calculated sub-codebooks, we quantize ECG signal within all bins of b_{1i}^S , $i \in \{0, 1, 2, \dots, 2^{N_1}\}$. The corresponding quantization indexes, denoted by I^s , are the final outputs of the compressor on the secondary sensor.

To assist our explanation, Fig. 9 presents a toy example of the conditional quantization method. In Fig. 9, the first three segments labeled with 1, 2, and 3 constitute a set. Near to the first set, the 5 numbers ($\{1, 2, 3, 4, 5\}$) labeled five segments form the second set. Beside the second one, the third set is constituted in the same way. Each of three sets ($\{1, 2, 3\}$, $\{1, 2, 3, 4, 5\}$ and $\{1, 2, 3, 4, 5\}$) covers the range of a b_{1i}^S , $i \in \{1, 2, 3\}$, and all the three sets cover the full dynamic range of x^S without overlapping. In each bin of b_{1i}^S , sub-codebook is calculated following the third step above. Then, the quantization is performed in each bin according to the calculated codebook and the numbers noted in Fig. 9 are the final results of the compression on the secondary sensor.

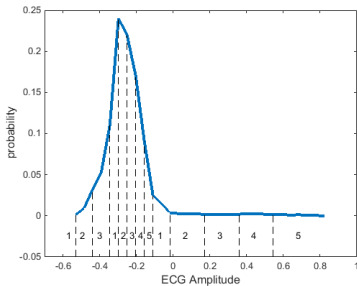


Fig. 9. Demon of compression on secondary ECG sensor

After the conditional quantization, the secondary sensor sends the quantization results to the primary sensor where the

reconstruction is performed. To reconstruct ECG signal at the decoder, two steps are needed.

- Among the set of sections $[x_i^P, x_{i+1}^P)$, $0 \leq i \leq 2^{N_1}$, we determine which section x^P belongs to. For example, x^P belongs to the k -th section, $x_k^P \leq x^P < x_{k+1}^P$.
- We take the k -th sub-codebook c_k^S to determine the reconstruction corresponding to the quantization index I^s .

Based on the description above, we can realize that there are N_2 bits used in the compression at the secondary sensor. In the experiments of this paper, we will show that N_2 is smaller than the number of bits for direction quantization, $N_2 < W$, where W denote the number of the bits used for direct quantization.

In this section, the structure of implementing the proposed ECG compression scheme is presented which is at low complexity and thus easy to be implemented at less hardware resource cost. Furthermore, the new compression scheme saves the consumed bits per sample. Indeed, besides the bits per sample, the sampling rate will also affect the accuracy of ECG compression and the hardware resource consumption. In the next section, we perform joint optimization with respect to the two aspects.

IV. TWO DIMENSIONAL BIT RATE OPTIMIZATION

In a remote health monitoring system, there are two factors significantly affecting the complexity and power consumption, the quantization bits per sample and and transmission period. Let W denote the average number of the bits used for quantizing each sample, and T_t is the period of transmitting the compressed ECG data. The bit rate r is calculated by $r = \frac{W}{T_t}$. In the optimization, our objective is to minimize average square error of the reconstructed ECG signal. The minimization is under the constraint of a given bit rate. With respect to the single dimension of bits number, the related minimization work refers to [20] The theoretic knowledge about the two-dimension optimization refers to [21]–[23].

For an ECG sensor, let T_0 denote the minimum sampling period. After the sampling, the ECG signal written as $x(mT_0)$, $m \in \mathbb{Z}$. In practice, the sampling frequency $\frac{1}{T_0}$ is over high for ECG signal. Thus, the ECG signal tor be transmitted should be down sampled. Let K denote the down sampling rate. After the down sampling, the ECG signal is transmitted. Therefore, we can realize that $T_t = KT_0$. Essentially, the optimization in this section is performed with respect to K and W .

A. Calculation of Bounds on T_t and W

1) *Upper bound on T_t* : In general cases, upper bound on sampling period is determined according to Nyquist sampling theorem. For sampling ECG signal, there are some differences.

ECG data is usually taken to assist diagnosis of cardiovascular diseases. In a heart beat period, a ECG signal consists of different waves, such as P wave, QRS wave and T wave. These waves provide assisting information for diagnosing different diseases. For example, ST segment depression or elevation accompanying with T wave inversion is used to diagnose myocardial infarction and cardiogenic shock. QRS voltage, ST-T wave, and R-wave changes are used to diagnose Cardiomyopathy.

We can easily realize that finer sampling is able to keep more information of ECG waveform. In general cases, durations of different waves are not the same in a ECG waveform. The wave having the smallest duration is most sensitive to sampling period. According to our observations, either Q-R segment or R-S segment has the smallest duration. Time interval between Q and R is denoted by t_{QR} . And interval between R and S is t_{RS} . To avoid information loss of QRS, we need to guarantee the smaller one between t_{QR} and t_{RS} is larger than the sampling period, $\min\{t_{QR}, t_{RS}\} \leq T_t$.

As mentioned before, ECG signals significantly changes for different people and different health conditions. Thus, we still use numerical method to investigate the smallest average duration of t_{QR} and t_{RS} . In the numerical analysis, we use ECG data published by Michael Oeff [24] for higher accuracy. The ECG data in [24] are sampled by 16 bits at the frequency of 10kHz. We estimate the durations of t_{QR} and t_{RS} of ECG data from 549 persons. According to our calculation, average value of t_{RS} is smaller than that of t_{QR} . Furthermore, from the 549 recordings, the smallest t_{RS} is equal to 56.9ms. Therefore, we need to guarantee sampling period T_t to provide the time resolution smaller than 56.9ms. Since sampling period of T_t generates resolution of $\frac{T_t}{2}$, the upper bound on T_t is 113.8ms, $T_t^U = 0.1138s$.

2) *Lower Bound on T_0* : The finer sampling generates the more accurate ECG signal while more hardware resources are consumed. In the joint optimization on bit rate, smallest sampling period at ADC is considered as the lower bound on T_0 . In our analysis, $1/360s$ is taken as the low bound on T_t , $T_t^L = \frac{1}{360}s$.

3) *Upper Bound on W* : Larger bit width means finer quantization which provides more accurate description on ECG amplitude. For a given wearable device, bit width W is upper bounded by the implementable largest number of quantization levels. The number of largest bits varies for different wearable devices. We consider 12 as the upper bound on W , $W^U = 12$.

4) *Lower Bound on W* : As introduced in Section IV-A1, waves in a beat rate period of ECG signal are used in diagnosing different types of diseases. These waves have different sensitivities to bit number. To determine lower bound on bit width W , we need to find out the wave which has the smallest peak average power ratio.

We still use data from [24] in the analysis of bit width lower bound. There are four steps in the calculation.

First, we select the ECG signals in which all waveform features can be observed by a doctor in medicine. The waveform features includes P, Q, R, S and T-waves.

Next, we measure the waves' summit-to-average distance, which are denoted by g_{Ξ} (Ξ includes an arbitrary member of the alphabet group $\{P, Q, R, S\}$). Essentially, g_{Ξ} is equal to the distance between the locally maximum point of each wave to the base of ECG signals. Companding with each element of g_{Ξ} , an envelope amplitude (distance between upper and lower envelope of a ECG recording) is measured. We use η_{Ξ} to denote the envelope amplitude companding with g_{Ξ} .

Third, at each ECG recording, we calculate the ratio of g_{Ξ} over its corresponding η_{Ξ} . The ratio is denoted by γ_k , $k \in \mathcal{K}$

where $|\mathcal{K}|$ is equal to the number of all calculated ratios.

Finally, the γ_k which has the smallest absolute value is selected to help us determine the lower bound on W . Let W^L denote the lower bound. We select W^L such that $\frac{1}{2^{W^L+1}} \leq \min(|\gamma_k|)$. According to our calculation, the lower bound on W is equal to 4, $W^L = 4$.

B. Joint Optimization on Bit Rate

At the wearable device, the quantized ECG data are transmitted to a data server for storage and analysis. We assume the time interval T_t is equal to KT_0 , $T_t = KT_0$. After receiving the quantized data, the data server reconstructs ECG signal. The reconstructed ECG data is denoted by \tilde{x} which is calculated as follows,

$$\tilde{x}(mT_0) = \sum_{n=-\infty}^{+\infty} \tilde{x}(nKT_0) \begin{bmatrix} u((m-nK)T_0) \\ -u((m-(n+1)K+1)T_0) \end{bmatrix}. \quad (26)$$

With the reconstructed ECG data \tilde{x} , we evaluate the reconstruction accuracy in terms of average square error which is denoted by ε . ε is calculated by

$$\varepsilon = \lim_{M \rightarrow \infty} \frac{1}{M} \sum_{m=-\frac{M}{2}+1}^{\frac{M}{2}} (x(mT_0) - \tilde{x}(mT_0))^2. \quad (27)$$

In the ECG data compression and transmission system, the bit rate budget is R which is essentially a upper bound on the actual bit rate r , that is,

$$r = \frac{W}{T_t} \leq R. \quad (28)$$

Under the constraint shown in (28), we minimize average square error in reconstructing the ECG signal. The optimization problem is formulated as

$$\begin{aligned} \text{minimize: } & \lim_{M \rightarrow \infty} \frac{1}{M} \sum_{m=-\frac{M}{2}+1}^{\frac{M}{2}} (c(mT_0) - \tilde{c}(mT_0))^2 \\ \text{subject to: } & \frac{W}{KT_0} \leq R \end{aligned} \quad (29)$$

In the optimization shown in (29), the variables include the average quantization number per sample (W) and the transmission period $T_t = KT_0$. Numerical methods are used to solve the optimization problem. Fig. 10 presents an example of solving optimization problem.

In Fig. 10 the colorful curves are contour of ε . The contours are plotted within a red dash rectangular. The boundaries of the rectangular is formed by the calculated bounds on W and T_t . The darker color means the smaller ε . The slope of a dot dash black lines are equal to an ideal bit rate budget R . A line with markers indicates the actual bit rate. Since W and K are both in discrete values, the actual bit rate lines with markers can hardly exactly match the ideal lines.

There two steps to determine the minimum MSE under the constraint of R . We first draw a bit rate budget line with the slope of R . Next, we find the contour curve which is tangent to the bit rate budget line. Then, the contour curve tangent to the budget line informs us the minimum MSE achievable at the bit rate of R .

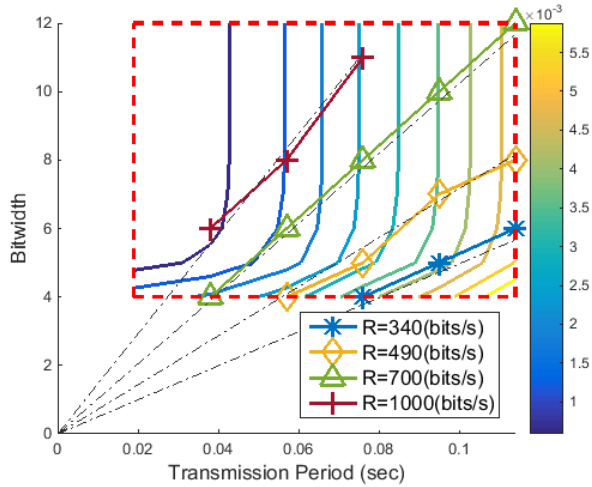


Fig. 10. ECG reconstruction ASE versus word length in bits and transmission period in second

V. EXPERIMENTAL VERIFICATIONS

In this section, experiments are performed to evaluate the effectiveness of the proposed method. We compare our method with existing ones in three aspects, computation complexity, ECG waveform distortion after reconstruction, and the efficiency of compression method in saving bits. Second, we investigate the performance of the conditional quantization at the secondary ECG sensor. Finally, experiments on joint bit rate optimization are performed.

In the experiments, our objective is to evaluate the effectiveness of proposed ECG compression method. In our knowledge, the compression is not as sensitive to the change of waveform shapes as the algorithms for R-wave detection or other cardiovascular disease diagnosis. Therefore, the experiments are performed on the data from only two databases, MIT-BIH Arrhythmia database [24] and European ST-T database [25].

A. Complexity and Reconstruction Accuracy Comparison

In this subsection, we investigate the performance of the proposed differential ECG compression method. To evaluate the performance, we compare our method with the ones in literature. The ECG compression schemes based on DCT and wavelet are considered since they are widely adopted in ECG compression. Different from pure wavelet algorithm, wavelet compression by the set partitioning in hierarchical trees algorithms is implemented. Since compressive sensing is widely discussed and applied, ECG signal is compressed via a compressive sensing algorithm. We also evaluate performance of two differential ECG compression methods, least mean square (LMS) based compression algorithm and DPCM based one.

Table I presents computation complexities of different ECG compression methods. Average numbers of multiplications, additions per data sample and required memory units are taken as the metrics. From Table I, DCT and wavelet based compressors need a large number of multiplications and memory units. The large number of multiplications are induced by the multiplication between ECG signal vector and groups

TABLE I
COMPARISON IN COMPUTATION COMPLEXITY

	Mul. (/sample)	Add. (/sample)	Memory U.
LMS	4	5	8
LMS (no. coef.)	4	5	8
DCT	39	1	1601
Wavelet+SPIHT	68	143	1216
Delta modulator	1	2	1
Compressive Sensing	212	183	2022
New method	0	3	2

of basis vectors. The volume of required multiplications is related to the length of a ECG segment. Besides the extensive demand on multipliers, a large number of memory units are also needed. LMS based compressor has lower computation complexity than the previous two compressors. From Table I, we can easily find that both DPCM based compressor and our method can be implemented in low complexity. Different from Delta modulator based compressor, our method does not need multiplication operations.

To present an intuitive impression on the performance of compression algorithms, we present the reconstructed ECG waveforms by all the mentioned algorithms. Due the page limits, the graphic performance comparison is performed on two ECG records, No. 112 record in MIT-BIH database and No. 103 record in European ST-T database. The reconstruction accuracy comparison for the two records are presented in Fig. 11 and Fig. 12 respectively. The computation is the compressions are performed in 8-bits numbers.

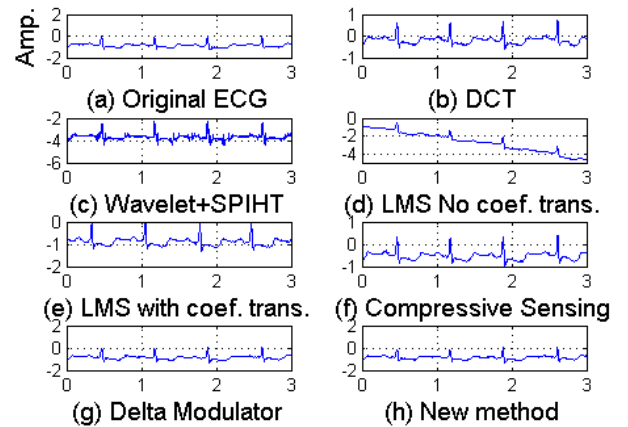


Fig. 11. Comparison of the reconstructions of No. 112 record in MIT-BIH arrhythmia database

From Fig. 11, the reconstruction ECG via the DCT based method retains the key features, such as P, Q, R, S, and T waves. Wavelet based compression incurs some noise-like distortion. In Fig. 11 (d), coefficients of adaptive filter are not updated and we can observe ECG waveform distortion. In Fig. 11 (e), the coefficients are adaptively updated which generate satisfying reconstruction accuracy. However, the bits used for updating coefficients are in a large number. The accuracy of the reconstructed ECG signal from the compress-

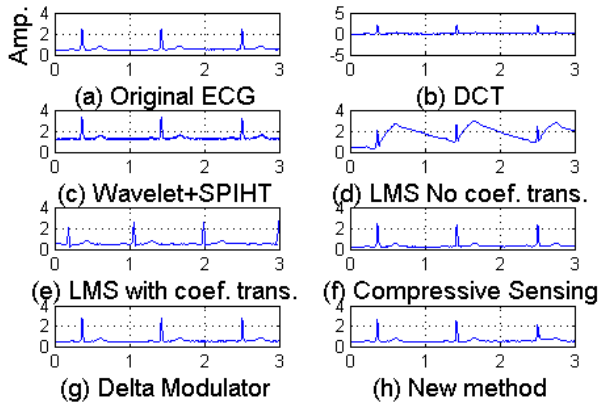


Fig. 12. Comparison of the reconstructions of No. 103 record in European ST-T database

sive sensing method is high while the computation burden is heavy. The key features of ECG signal can also be observed in DPCM based compressor (Fig. 11 (g)). However, we can find unexpected fluctuations between R and S. DPCM quantizes the error occurring estimating current ECG value. When ECG waveform changes fast, such as in the segment between R and S, DPCM is not able to keep tracking of the fast change. Thus, the unexpected fluctuations occur. Our method quantizes the ECG amplitude change directly. Thus, our method is more robust to the fast change. The similar phenomena can also be observed in Fig. 12.

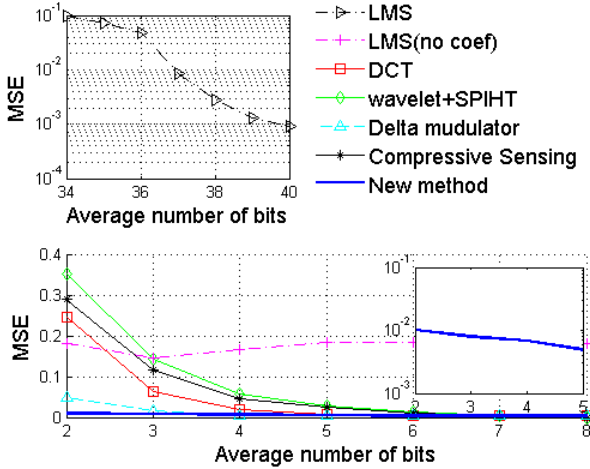


Fig. 13. MSE versus average number of bits per sample for records in MIT-BIH arrhythmia database

Fig. 11 and Fig. 12 illustrate the reconstructed ECG waveform at a fixed bit width of 8. Furthermore, we present the normalized MSE of the reconstructed ECG at different bit widths in Fig. 13 and Fig. 14 which curves are calculated from the records in MIT-BIH Arrhythmia database and European ST-T database respectively. From Fig. 13, wavelet based compression induces the worst reconstruction accuracy. When 4 coefficients of LMS filters are not transmitted from a compressor, MSE does not decrease with bit number increasing. When

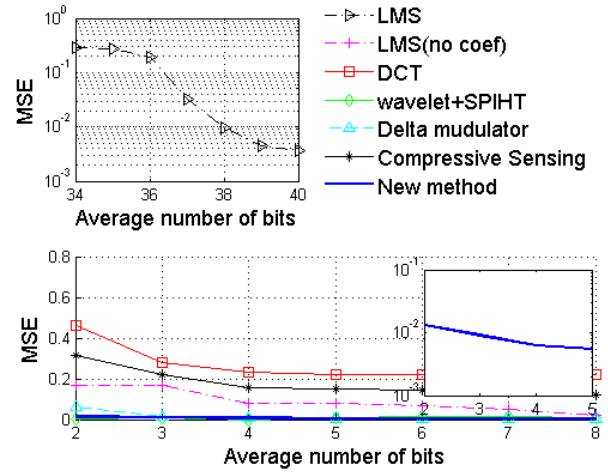


Fig. 14. MSE versus average number of bits per sample for records in European ST-T database

the coefficients are transmitted, MSE decreases significantly with bit width increasing. However, the coefficient updating requires more bits. Our new method achieve the smallest MSE at a given low bit rate. The advantage of the new method over the existing ones can also be observed in Fig. 14.

B. Simulation in Double Sensors Based ECG Compression

In this subsection, we investigate the performance of double sensors based ECG compression method. As discussed in previous sections, the distribution of ECG signal from primary sensor is priorly known by the secondary sensor. Thus, conditional quantization can be performed at the secondary sensor. The quantization results are transmitted to the primary sensor via a perfect channel. The primary sensor differentially quantize ECG signal acquired by itself. The results of conditional quantization and differential quantization are transmitted to a remote data center. At the data center, the ECG signal acquired by the primary sensor is first reconstructed. Then, reconstruction of the ECG signal from the secondary sensor is performed.

The combination of differential quantization at primary sensor and the conditional quantization at the secondary sensor is called as hybrid quantization structure. For comparison, we also consider other two quantization structures in the double sensors based compression. First, differential quantization is applied in both primary and secondary sensors. Second, differential quantization is taken at the primary sensor and uniform quantization used at the secondary one. The average MSE of the reconstructed ECG at both the primary and secondary sensors is taken as the accuracy metric.

The results of the two sensors based ECG compression are presented in Fig. 15. From the results, the proposed hybrid quantization method outperforms other two, the conventional quantization on original ECG signal (labeled as 'uniform quantization') and the two-independent-differential ECG quantization (labeled as 'twice diff. str'). The advantage of the proposed two sensors based compression scheme is caused by the reduction of redundant information between ECG signal

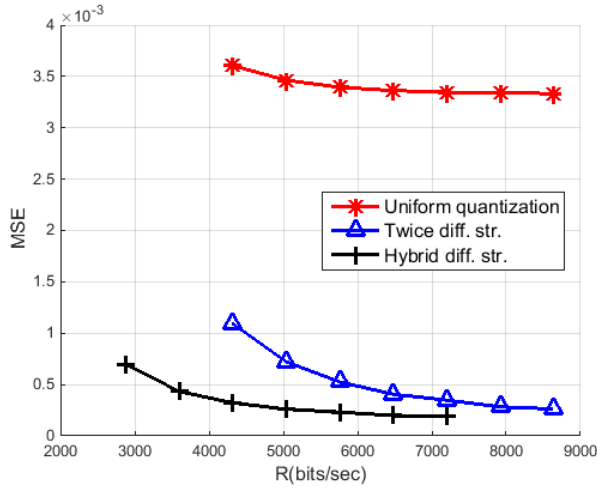


Fig. 15. Bit rate in ECG compression on double sensors from the two sensors.

C. Simulation in Joint Bit Rate Optimization

Until now, the simulations are performed in the precondition that the sampling period is fixed. In this subsection, we investigate the performance of joint bit rate optimization over quantization bit number and transmission period. As a comparison, quantization results are transmitted at a period of $1/360s$ which is the same with the sampling period for the records in MIT-BIH database. Via interpolation, the equivalent sampling at $360Hz$ is also performed on the data records for European ST-T database.

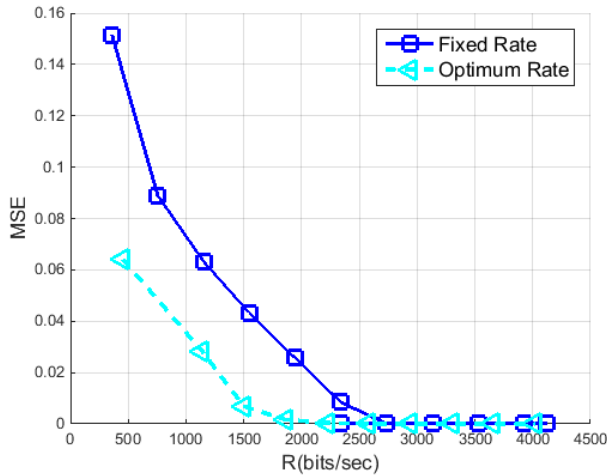


Fig. 16. Joint bit rate optimization

Fig. 16 plots ‘MSE-bit rate’ curves with and without the joint optimization. The two dimensional optimization is constrained by the bounds both in sampling period and quantization bits per sample. These bounds, which are calculated in Section IV-A, enable us guarantee key features of ECG signal can be retained in the compression. From Fig. 16, advantage

of the joint optimization on saving bit rate can be clearly observed.

VI. CONCLUSION

We investigate the compression of ECG signal which is important for saving hardware and power consumption in health telemonitoring systems. Different from the ECG compression work in literature, compression scheme based on multiple ECG sensors is considered. Without loss of generality, we consider an example in which there are two ECG sensors, a primary and a secondary ECG sensor. At the primary one, we use a novel differential structure to compress ECG signal which effectively reduces the redundant information between adjacent ECG samples. At the secondary ECG sensor, conditional quantizer is proposed to compress ECG signal which utilizes the inherent connection between the shapes of ECG signals from the two sensors. Experiments verify the advantage of our proposed compression scheme both in complexity and reconstruction accuracy.

REFERENCES

- [1] Y. B. Lin, Y. W. Lin, C. M. Huang, C. Y. Chih, and P. Lin, “Tottalk: A management platform for reconfigurable sensor devices,” *IEEE Internet of Things Journal*, vol. PP, no. 99, pp. 1–1, 2017.
- [2] P. Huang and Y. Pi, “An improved location service scheme in urban environments with the combination of gps and mobile stations,” *Wireless Communications and Mobile Computing*, vol. 14, no. 13, pp. 1287–1301, 2014. [Online]. Available: <http://dx.doi.org/10.1002/wcm.2232>
- [3] —, “Wireless internet assisting satellite position in urban environments,” in *2011 6th International ICST Conference on Communications and Networking in China (CHINACOM)*, Aug 2011, pp. 262–267.
- [4] J. Pandey and B. Otis, “A sub-100 μW mics/ism band transmitter based on injection-locking and frequency multiplication,” *Solid-State Circuits, IEEE Journal of*, vol. 46, no. 5, pp. 1049–1058, May 2011.
- [5] J. Ma, T. Zhang, and M. Dong, “A novel ecg data compression method using adaptive fourier decomposition with security guarantee in e-health applications,” *IEEE Journal of Biomedical and Health Informatics*, vol. 19, no. 3, pp. 986–994, May 2015.
- [6] T. Marisa, T. Niederhauser, A. Haeberlin, R. A. Wildhaber, R. Vogel, M. Jacomet, and J. Goette, “Bufferless compression of asynchronously sampled ecg signals in cubic hermitian vector space,” *IEEE Transactions on Biomedical Engineering*, vol. 62, no. 12, pp. 2878–2887, Dec 2015.
- [7] C. Deepu and Y. Lian, “A joint QRS detection and data compression scheme for wearable sensors,” *Biomedical Engineering, IEEE Transactions on*, vol. 62, no. 1, pp. 165–175, Jan 2015.
- [8] A. Bendifallah, R. Benzid, and M. Boulemden, “Improved ECG compression method using discrete cosine transform,” *Electronics Letters*, vol. 47, no. 2, pp. 87–89, January 2011.
- [9] A. Bilgin, M. Marcellin, and M. Altbach, “Compression of electrocardiogram signals using JPEG2000,” *Consumer Electronics, IEEE Transactions on*, vol. 49, no. 4, pp. 833–840, Nov 2003.
- [10] Z. Lu, D. Y. Kim, and W. Pearlman, “Wavelet compression of ECG signals by the set partitioning in hierarchical trees algorithm,” *Biomedical Engineering, IEEE Transactions on*, vol. 47, no. 7, pp. 849–856, July 2000.
- [11] Y. Zou, J. Han, S. Xuan, S. Huang, X. Weng, D. Fang, and X. Zeng, “An energy-efficient design for ECG recording and R-peak detection based on wavelet transform,” *Circuits and Systems II: Express Briefs, IEEE Transactions on*, vol. 62, no. 2, pp. 119–123, Feb 2015.

- [12] L. Polania, R. Carrillo, M. Blanco-Velasco, and K. Barner, "Exploiting prior knowledge in compressed sensing wireless ECG systems," *Biomedical and Health Informatics, IEEE Journal of*, vol. 19, no. 2, pp. 508–519, March 2015.
- [13] V. Cambareri, M. Mangia, F. Pareschi, R. Rovatti, and G. Setti, "A case study in low-complexity ecg signal encoding: How compressing is compressed sensing?" *IEEE Signal Processing Letters*, vol. 22, no. 10, pp. 1743–1747, Oct 2015.
- [14] H. Mamaghanian, N. Khaled, D. Atienza, and P. Vanderghelynst, "Compressed sensing for real-time energy-efficient ecg compression on wireless body sensor nodes," *IEEE Transactions on Biomedical Engineering*, vol. 58, no. 9, pp. 2456–2466, Sept 2011.
- [15] U. E. Ruttimann and H. V. Pipberger, "Compression of the ECG by prediction or interpolation and entropy encoding," *Biomedical Engineering, IEEE Transactions on*, vol. BME-26, no. 11, pp. 613–623, Nov 1979.
- [16] C.-C. Sun and S.-C. Tai, "Beat-based ECG compression using gain-shape vector quantization," *Biomedical Engineering, IEEE Transactions on*, vol. 52, no. 11, pp. 1882–1888, Nov 2005.
- [17] S.-L. Chen and J.-G. Wang, "VLSI implementation of low-power cost-efficient lossless ECG encoder design for wireless healthcare monitoring application," *Electronics Letters*, vol. 49, no. 2, pp. 91–93, January 2013.
- [18] G. Einarsson, "An improved implementation of predictive coding compression," *Communications, IEEE Transactions on*, vol. 39, no. 2, pp. 169–171, Feb 1991.
- [19] S. Lloyd, "Least squares quantization in PCM," *Information Theory, IEEE Transactions on*, vol. 28, no. 2, pp. 129–137, Mar 1982.
- [20] P. Huang and D. Rajan, "Estimation of centralized spectrum sensing overhead for cognitive radio networks," in *2014 IEEE 25th Annual International Symposium on Personal, Indoor, and Mobile Radio Communication (PIMRC)*, Sept 2014, pp. 659–663.
- [21] —, "Bounds on the overhead of spectrum sensing in cognitive radio," in *2014 IEEE Global Communications Conference*, Dec 2014, pp. 846–850.
- [22] P. Huang, Y. Du, and Y. Li, "Stability analysis and hardware resource optimization in channel emulator design," *IEEE Transactions on Circuits and Systems I: Regular Papers*, vol. 63, no. 7, pp. 1089–1100, July 2016.
- [23] P. Huang, W. Wang, and Y. Pi, "Estimation on channel state feedback overhead lower bound with consideration in compression scheme and feedback period," *IEEE Transactions on Communications*, vol. 65, no. 3, pp. 1219–1233, March 2017.
- [24] A. L. Goldberger, L. A. N. Amaral, L. Glass, J. M. Hausdorff, P. C. Ivanov, R. G. Mark, J. E. Mietus, G. B. Moody, C.-K. Peng, and H. E. Stanley, "PhysioBank, PhysioToolkit, and PhysioNet: Components of a new research resource for complex physiologic signals," *Circulation*, vol. 101, no. 23, pp. e215–e220, 2000 (June 13), circulation Electronic Pages: <http://circ.ahajournals.org/cgi/content/full/101/23/e215> PMID:1085218; doi: 10.1161/01.CIR.101.23.e215.
- [25] —, "Physiobank, physiotoolkit, and physionet," *Circulation*, vol. 101, no. 23, pp. e215–e220, 2000. [Online]. Available: <http://circ.ahajournals.org/content/101/23/e215>